Optimal Control–Based Modeling of Cyclist Behavior

Xinyu Zhang*[1] and Meng Wang[1]

[1]Chair of Traffic Process Automation, Technische Universität Dresden, Germany

SHORT SUMMARY

Bicycles share similarities with motorised vehicles in that their primarily longitudinal movement is limited by kinematic constraints, but they are more flexible in lateral motion and less restricted by lane discipline. While a few models for cycling were reported in the literature, they mostly explain specific behaviours under disconnected assumptions. A comprehensive cycling behavior model that can simulate primary cyclist behaviors, including lane-keeping, turning, and obstacle avoidance, is still lacking. This paper develops an optimal control-based model to simulate cyclist's tactical and operational behaviors, assuming cyclist minimizes accumulated costs anticipated in a finite future. This finite future can be in time, e.g. when cycling on a long stretch or in space, e.g. when turning or approaching a red light. The costs considered by cyclists reflect multicriteria of travel efficiency, traffic rules, safety. Numerical experiments are conducted to check the plausibility of the model and the influence of key parameters.

Keywords: cyclist behavior, optimal control theory, tactical and operational behavior.

1 INTRODUCTION

Cycling is an active traffic mode with great potential for achieving sustainability goals. Compared to drivers, cyclists are less confined by infrastructure, exhibiting much flexibility in utilizing road space and navigation. Meanwhile, there is significant heterogeneity in cyclist behaviors and performance, highlighting the diverse range of experiences and motivations among riders (Hoogendoorn & Daamen, 2016). Understanding and predicting cyclist behavior, especially how they make decisions for trajectory planning and control their bicycles at the tactical and operational levels, are crucial for policy-making, infrastructure design and traffic management.

Existing cyclist models in the literature mostly resort to the adaptation of either vehicle driver behavior models or the pedestrian behavior models (Twaddle et al., 2014). One modelling approach is to divide the lane into several smaller strips, utilizing car-following models as longitudinal models and utilizing a discrete lane choice model to select the strip within the lane (Mathew et al., 2012). To adapt the time- and space-discrete cellular automata (CA) models to bicycles, Yao et al. (2009) designed smaller cells for multiple road users to allow them to occupy more than one cell per time step. These models adapted from vehicles can not simulate continuous lateral movements.

Apart from this, pedestrian behavior models like Social Force Models (SFMs) (Helbing & Molnar, 1995) are less bound by lane discipline and less rule-oriented. They can simulate the flexible motion planning of cyclist in the 2D plane but do not consider the dynamic constraints of cycling. To solve this issue, Schmidt et al. (2023) developed a microscopic model describing bicycle interaction using SFMs with consideration of bicycle kinematics. However, they do not capture the tactical decisions of cyclists. Schönauer et al. (2012) added a tactical force vector based on the Stackelberg game concept to their social force model to model all road user's movements in a shared zone, the sum of the partial payoffs for both road users is used as a strategy. Hoogendoorn et al. (2021) developed a game theoretical framework that includes different strategies (cooperative, zero-acceleration, demon opponent) including traffic rules considering the communication between cyclists. While gaming nature is relevant in scenarios with clear and opposing conflicts, cyclists often exhibit non-strategic behavior (e.g., following habitual routes or relying on instincts).

The contribution of the paper is to model cycling behavior under an optimal control framework. Cyclists are assumed to be predicted cost minimizers: they predict the future based on a two-dimensional (2D) kinematic model and choose steering angle and acceleration to minimize some

cost function in a finite future. The costs considered by cyclists include travel efficiency cost, lane-keeping costs, safety cost, physical effort cost, and cost due to undesired situations at the final time of the finite future. Heterogeneity and individual preferences can be reflected by the weights of different costs. The use of the 2D kinematic model ensures that longitudinal and lateral bicycle movements are coupled and realistic bicycle dynamics constraints are respected in simulation. The tactical decisions of cyclist (e.g., avoidance strategies and deceleration patterns) are implicitly embedded in the results of the optimized trajectory. Face validation and analysis of the model outcomes are performed to clarify how the observed phenomena depend on parameter settings.

2 Optimal cyclist's behavior model formulation

In this section, the conceptual design, the theoretical assumption and the mathematics model of cyclist's behavior are introduced.

Conceptual Model and Assumptions

Twaddle et al. (2014) adapted driver behavior classification (Michon, 1985) to cyclist areas, where strategic behavior includes choice of route and departure time, tactical behavior includes decisions and operations, and operational behavior includes control of bicycle. Our model focuses on the tactical layer behaviour as shown in subfigure 1a. Our model considers bicycle's kinematics, integrates inputs from the strategy layer with cyclist's objectives and preferences, as well as environmental observations, such as information on obstacles and infrastructure. The result of the trajectory optimization can serve as reference trajectory to an operational layer that controls bicycle dynamics.

We assume cyclists plan their trajectories in the finite future based on individual travel objectives, interaction preferences, and physical riding capabilities. Such objectives can include:

- minimizing deviation from the desired heading,
- minimizing deviation from the desired lane position,
- minimizing deviations from the desired speed or minimizing travel time,
- maximizing safety and/or minimizing risk.
- maximizing smoothness and comfort and/or minimizing physical efforts.

We categorize the cyclist trajectory planning approach into two approaches: one approach involves trajectory planning over a finite time horizon where the route lacks a specific, predefined destination (e.g. the green cyclist in subfigure 1b), and the other plans future trajectory to a target point in space, e.g. in turning and stopping scenarios (blue cyclists in subfigure 1b). Such differentiation allows us to model primary behaviors of different scenarios under a unified mathematical framework, as we will show in the ensuing of this section.

Kinematic Motion of Cycling

We utilize the unicycle model to simulate the kinematic motion of cycling, effectively capturing cyclist's behavior by coupling longitudinal and lateral movements (Fig. 2). This model strikes a balance between realism and simplicity. Compared to the more complex multi-body model, which involves intricate dynamics of interconnected rigid bodies and significantly higher computational demands, the unicycle model is computationally efficient. Apart from this, the simpler mass-point model represents cyclist as one single point and lacks rotational dynamics, limiting its ability to represent realistic cycling behavior. Four state variables of cyclists are shown in Eq. 1.

$$\mathbf{x}(t) = [x(t), y(t), \theta(t), v(t)] \tag{1}$$

where $\mathbf{x}(t)$ denotes the state of a bicycle at time t; $x(t)$ and $y(t)$ are the global plane coordinate of the bicycle in m; $\theta(t)$ is the heading angle in rad; v is the velocity in m/s. The control variable is defined as in Eq. 2:

$$\mathbf{u}(t) = [a_l(t), w(t)] \tag{2}$$

Here, $a_l(t)$ and $w(t)$ represent the cyclist's pedaling and steering actions, corresponding to longitudinal and lateral control, respectively.

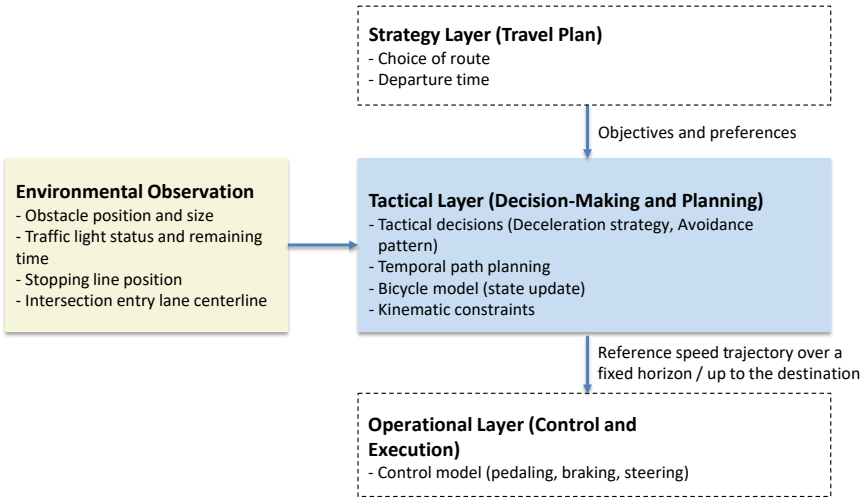

(a) Conceptual model framework

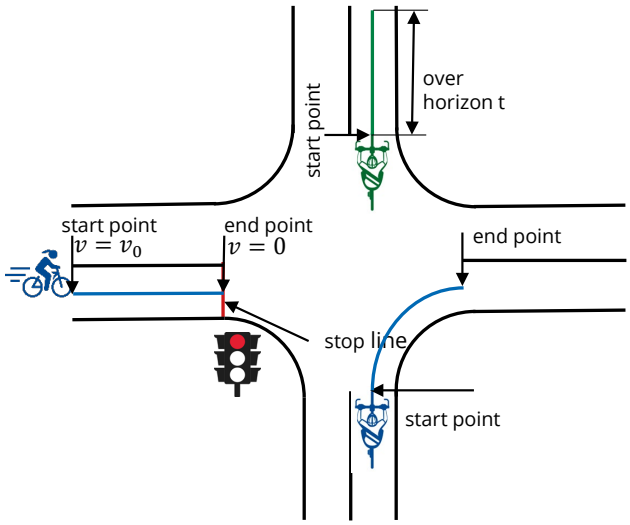

(b) Scenarios of cyclist trajectory planning

Figure 1: Conceptual framework

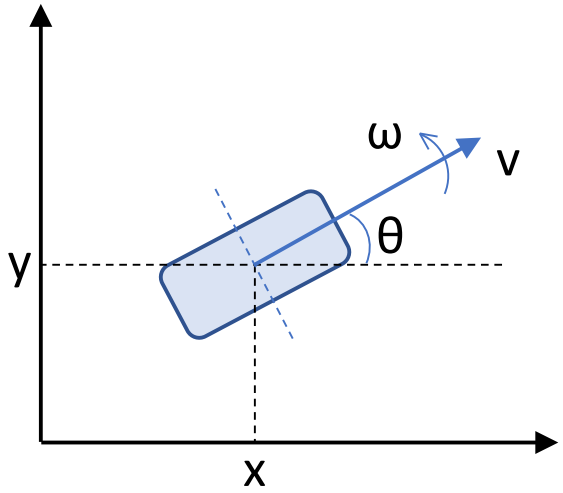

Figure 2: Unicycle model

The state dynamics is described in Eq. 3.

$$\frac{d\mathbf{x}(t)}{dt} = \frac{d}{dt}\begin{bmatrix} x(t) \\ y(t) \\ \theta(t) \\ v(t) \end{bmatrix} = \begin{bmatrix} v(t)\cos(\theta(t)) \\ v(t)\sin(\theta(t)) \\ \omega(t) \\ a_l(t) \end{bmatrix} \tag{3}$$

Realistic constraints on velocity (Eq. 4), acceleration (Eq. 5), and angular velocity (Eq. 6) are imposed to ensure they remain within reasonable ranges, considering the physical limits of human cycling capabilities and bicycle characteristics. The maximum centripetal acceleration is given by $a_{cmax} = \mu g$, where μ represents the coefficient of friction and g is the acceleration due to gravity (Eq. 7).

$$v_{min} \leq v(t) \leq v_{max} \tag{4}$$

$$a_{lmin} \leq a_l(t) \leq a_{lmax} \tag{5}$$

$$w_{min} \leq w(t) \leq w_{max} \tag{6}$$

$$w(t)v(t) \leq a_{cmax} \tag{7}$$

Two Finite Future Formulations

Model Over a Fixed Time Horizon

This framework applies to scenarios where no obvious target point is within the cyclist's line of sight. The process objectives of riders over target horizon T are defined as Eq.(8), including operation costs L_{op}, which describe physical efforts that riders make to change the motion state, safety costs L_s, when facing obstacles, and lane deviation cost L_{lane}, representing compliance with the "stay within lane" rule. The square of deceleration a_{dec} , acceleration a_{acc}, and centripetal acceleration a_c are related to the operation costs L_{op} (Eq.(9) to Eq.10). Specifically, the fourth power dependence results in an accelerated increase in L_l for values of $y(t)$ farther from the center. y_c and w_l devote center line location and width of bicycle lane. This characteristic makes the function suitable for modeling lane rules where a sharp response is required in objective functions as the cyclist moves away from the lane (subfigure 3a). Eq.(12) represents the terminal cost Φ_1 based on desired velocity v_d and desired heading θ_d.

$$L(\mathbf{x}, \mathbf{u}) = \int_{t=0}^{t=T} (L_{op} + L_s + L_l)\, dt + \Phi_1(\mathbf{x}(T)) \tag{8}$$

$$L_{op} = \beta_1 a_l^2 \Delta(-a_l) + \beta_2 a_l^2 \Delta(a_l) + \beta_3 a_c^2 \tag{9}$$

$$\Delta(x) = \begin{cases} 1, & \text{if } x >= 0 \\ 0, & \text{if } x < 0 \end{cases} \tag{10}$$

$$L_l = \beta_5 \cdot \left(1 + \left(\frac{2(y(t) - y_c)}{w_l}\right)^4\right) \tag{11}$$

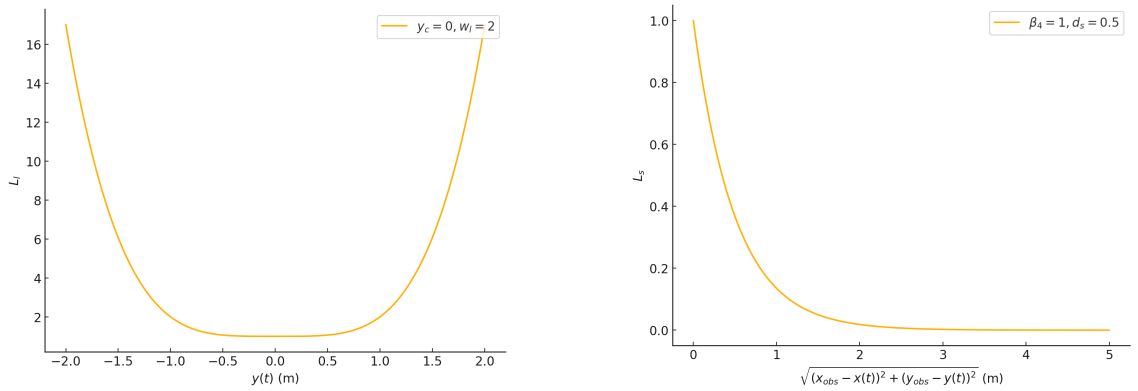

(a) Lane deviation cost L_l (Eq.11)

(b) Safety cost L_s (Eq.13)

Figure 3: Function L_l and function L_s

$$\Phi_1(\mathbf{x}(T)) = \beta_6(v(T)) - v_d)^2 + \beta_7(\theta(T)) - \theta_d)^2 \tag{12}$$

When no obstacles are present in the line of sight, safety cost L_s equals zero. L_s can be extended to incorporate obstacle-avoidance behaviors when encountering stationary obstacles. L_s are determined by the position of obstacles (x_{obs}, y_{obs}), the optimized position of cyclist ($x(t)$), $y(t)$), and

the dimension of obstacles with average radius d_s (Eq.13). When the distance is less than $d_s, 0.5$ meters, the function exhibits exponential growth, indicating an increased safety cost as the cyclist approaches the obstacle (Subfigure 3b).

$$L_s(t) = \beta_4 \exp\left(-\frac{\sqrt{(x_{obs} - x(t))^2 + (y_{obs} - y(t))^2}}{d_s}\right) \tag{13}$$

Model with Fixed Destination

This model can simulate cyclist behavior in scenarios with a fixed destination. We use this model to simulate behavior in scenarios involving a deceleration process at a fixed stop line and turning behavior at an intersection. We add L_e (Eq. 15) in the process objective functions to represent the constraint on cycling time in situations involving turns with limited time and stopping when encountering a red light (Eq. (14)). Soft constraints $\Phi_2(\mathbf{x}(T))$ regarding the difference between the terminal state $\mathbf{x}(T)$ and the desired terminal state $\mathbf{x}_d = [x_d,\ y_d,\ \theta_d,\ v_d]$ are included in the objective functions (Eq. 17).

$$L(\mathbf{x}, \mathbf{u}) = \int_{t=0}^{t=t_{opt}} (L_{op} + L_e + L_v)\, dt + \Phi_2(\mathbf{x}(T)) \tag{14}$$

$$L_e(t) = \beta_8 * 1 \tag{15}$$

$$L_v(t) = \beta_9(v(T)) - v_d)^2 \tag{16}$$

$$\Phi_2(\mathbf{x}(T)) = \beta_9((\theta(T) - \theta_d)^2 + (x(T) - x_d)^2 + (y(T) - y_d)^2) \tag{17}$$

Solution

IPOPT (Interior Point Optimizer) solver (Wächter & Biegler, 2006) is ultilized in our case based on the primal-dual interior point method, which is specifically designed to handle large-scale nonlinear programming (NLP) problems. Its optimizes iteratively the problem to find an optimal solution that satisfies the Karush-Kuhn-Tucker (KKT) conditions. We use the open source framework CasADi (Andersson et al., 2019) to solve the problems mentioned above.

$$\begin{aligned} \text{minimize:} \quad & L(\mathbf{x}, \mathbf{u}) \\ \text{subject to:} \quad & u_{\text{lb}} \leq \mathbf{u} \leq u_{\text{ub}}, \\ & g_{\text{lb}} \leq g(\mathbf{x}, \mathbf{u}) \leq g_{\text{ub}} \end{aligned} \tag{18}$$

$\mathbf{u} \in R^{n_x}$ devotes the decision variable. $L(\mathbf{x}, \mathbf{u})$ is formulated in Eq. 8 and Eq. 14. Apart from known partameters and bounds (lbu, ubu, lbg ubg), the initial guess for the decision variables are provided for the primal-dual solution. Convergence Tolerance is set to 10^{-6} to achieve accurate results.

3 Experimental Design

Table 1 shows the experiments designed to simulate cyclist's behaviors in varying scenarios.

Lane-keeping Scenarios

The first aim of the experiments in this scenario is to investigate how cyclists with varying tendencies (β_5) to return to the desired lane position plan their trajectories over a 5 second-fixed-horizon. At this point, we simulated a one-way lane with a width of 1.5 m, assuming that the cyclist aims to stay as close to the center of the lane as possible based on Eq. 11. An initial offset (0, 2) from the center line will be set as control parameter. Additionally, the desired speed will be set as the initial speed 4m/s to eliminate the influence of acceleration and deceleration processes on the curve. It is modeled based on model over fix horizon.

Apart from this, a deceleration experiment is designed to explore how the factor of the deceleration-related cost component (β_1) influences the deceleration process. Model with fix destination is utilized in this experiment to simulate the deceleration response to a red light with the requirement to stop at a fixed stop line.

Scenario	Goal	Independent Parameter	Control Parameter	Assessment Metrics
Lane-keeping (straight)	Exploring how cyclists with different desire to return to the centerline influence the trajectory	β_5	v_d, $\mathbf{x}(0)$, T	Trajectory, speed, acceleration
	Exploring how the cyclists with different operational skill levels influence the speed (deceleration)	β_1	v_d, $\mathbf{x}(0)$, $\mathbf{x}_d$	Speed, deceleration
Turning	Exploring the changes in cycling speed along the trajectory under different turning radii	x_d, y_d	$\mathbf{x}(0)$, θ_d, v_d	Trajectory, speed, acceleration
	Exploring the changes in cycling speed along the trajectory under different initial speed	v_0	$x(0)$, $y(0)$, $\theta(0)$, v_d, $\mathbf{x}_d$	Trajectory, speed, acceleration
Stationary obstacle avoidance	Exploring how cyclists with different operation skill levels and varying levels of safety awareness on obstacles plan their avoidance trajectory	β_3, β_4	x_{obs}, y_{obs}, d_s, v_d, $\mathbf{x}(0)$, T	Lateral deviation
	Exploring how the capacity of cyclists to tolerate rule violations when crossing solid or dashed lines influence the trajectory	β_5	x_{obs}, y_{obs}, d_s, v_d, $\mathbf{x}(0)$, T	Trajectory

Table 1: Experimental design in different scenarios

Turning Scenarios

To investigate cyclists behavior during turns, we utilize model with fixed destination since the center point of the turning lane can be pre-defined as the target destination. In particular, we focus on the coupling relationship between linear velocity, angular velocity, and turning radius. We explore the changes in cycling speed along the trajectory under different turning radii and initial velocities. Terminal states are limited by soft constraints. In order to better observe the speed-changing process during turning, velocity cost L_v from Eq. 16 is defined as zero in this scenario and L_e from Eq. 15 serve as the efficiency cost during turns.

Stationary Obstacle Avoidance Scenarios

Among the various maneuvers performed by cyclist, obstacle avoidance has gained significant attention due to safety concerns. We investigate how cyclist with differing levels of operational skill and varying levels of safety awareness on obstacle plan the trajectory. Model over fix horizon is utilized for this scenarios.

4 RESULTS AND DISCUSSION

Lane-keeping Scenarios

Fig. 4 demonstrates the impact of varying β_5 values on the optimal trajectory. As β_5 increases, the cost of deviation from center line becomes larger, resulting in a less smooth trajectory. The change in linear velocity is simultaneously influenced by both the centripetal acceleration term and the linear acceleration term in the cost function. The angular velocity ω and linear velocity v exhibit opposing trends under maximum centripetal acceleration a_c, which is $9.81 m/s^2$ for dry floor (purple dashed line). Due to the constraint of the expected terminal velocity, the speed returns to 4 m/s in the end (Fig. 5).

In deceleration scenarios, the factor β_1 represents the proportion of deceleration operation cost. When β_1 reaches 100, the result shows uniform deceleration with purple line in Fig. 6. With smaller β_1 values, the result shows maintaining speed until near the stop line, followed by a sudden deceleration, which models cyclist with a higher tolerance for braking discomfort, resulting in shorter duration for the deceleration process.

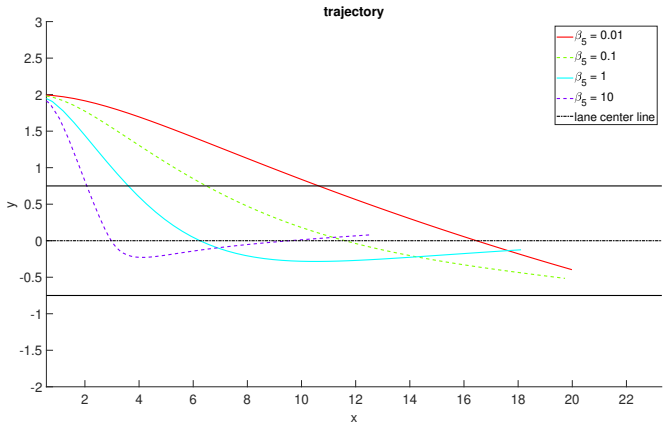

Figure 4: Optimal trajectory results for lane-keeping scenario with different β_5 ranging from 0.01 to 10

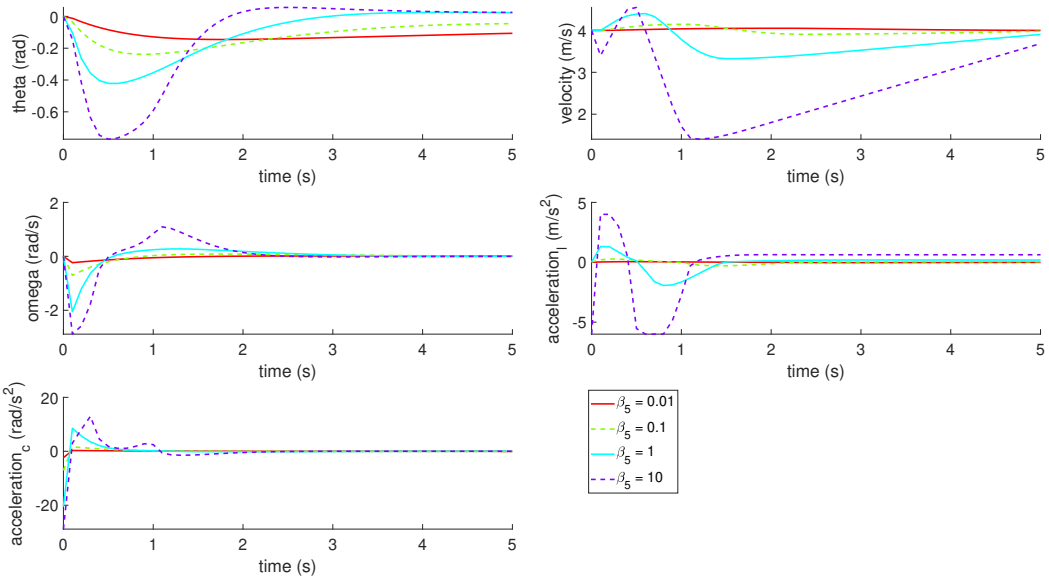

Figure 5: State variables results for lane-keeping scenario with different β_5 ranging from 0.01 to 10

Turning

Fig.7 first shows the optimized trajectorys of a cyclist from (0,0) to different endpoints, (1,1)(solid line) with a smaller radius and (7,7) (dashed line) with a larger radius. Different colors represent cyclists with different initial speed. With a larger turning radius and less angular changes, the velocity generally remains constant (dashed lines) (Fig.8). Meanwhile, cyclists with the closer destination of (1,1) decelerate their linear speed as the angular velocity increases during small turns due to the upper limit of the centripetal acceleration $4m/s^2$ (wet floor). Cyclist with higher initial speeds of $4m/s$ reaches this limit (blue solid line). Notably, the centripetal acceleration reaches zero once, when the angular velocity decreases to zero and then reverses direction while the linear speed approaches zero. This behavior occurs due to the high initial speed, which causes the cyclist to overshoot the y-axis position.

Stationary Obstacle Avoidance

We introduce β_4 as a representation of an individual's alertness and safety awareness of cyclists by cycling near obstacles. β_3 can represent the cyclist's tolerance of discomforts from centripetal force and operational cost during turns. Fig. 9 illustrates the combined effects of β_3 and β_4 on optimised

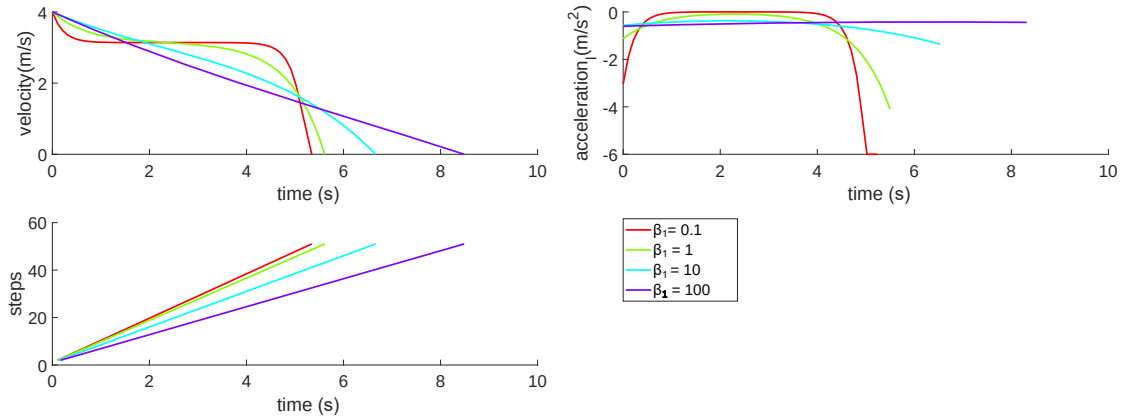

Figure 6: Optimal trajectory results for deceleration scenario with different β_1 ranging from 0.01 to 10

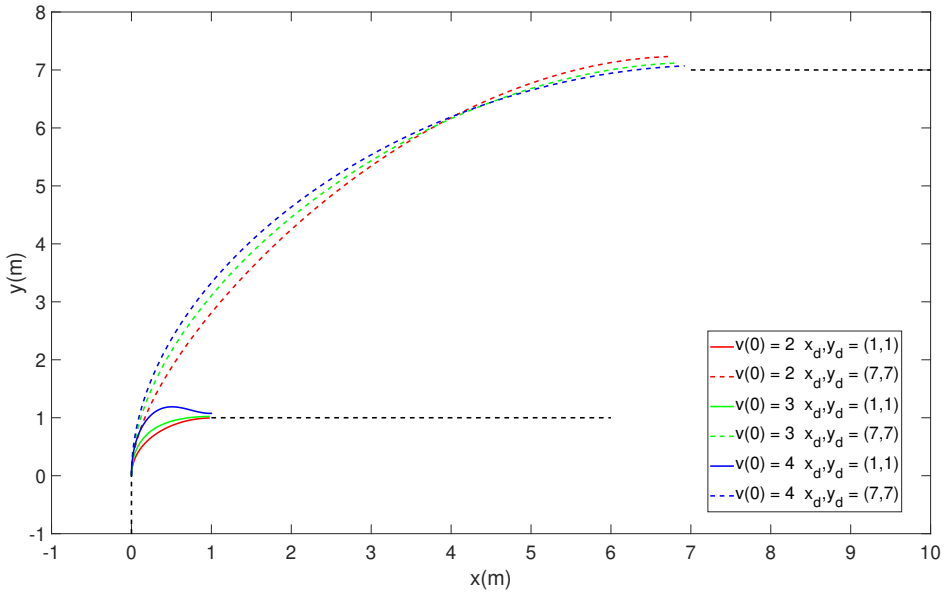

Figure 7: Optimal trajectory results for turning scenarios with different initial speeds and radii

trajectory planning. Our results show that the maximum deviation from the center line increases with an increase in β_4, indicating a tendency to keep larger distance with obstacles at (5,0). Conversely, as β_3 increases, the maximum deviation decreases, reflecting a reduced willingness of cyclists to move away from the centerline. The results indicate that both β_3 and β_4 independently influence the trajectory planning of the bicycle.

Fig. 10 illustrates the varying capacities of cyclist to tolerate rule violations when crossing solid lane boundaries, represented by larger β_5 (blue line), or dashed lane boundaries, represented by smaller β_5 (red). Different avoidance patterns are depicted in a complex obstacle avoidance scenario, where the safety cost and steering operation cost are balanced against adherence to lane-keeping rules.

5 CONCLUSIONS

In this paper, a comprehensive cyclist behavior model based on optimal control theory is developed to simulate tactical cyclist trajectory planning. assuming cyclist minimizes accumulated costs anticipated in a finite future. This finite future can be in time, e.g. when cycling on a long

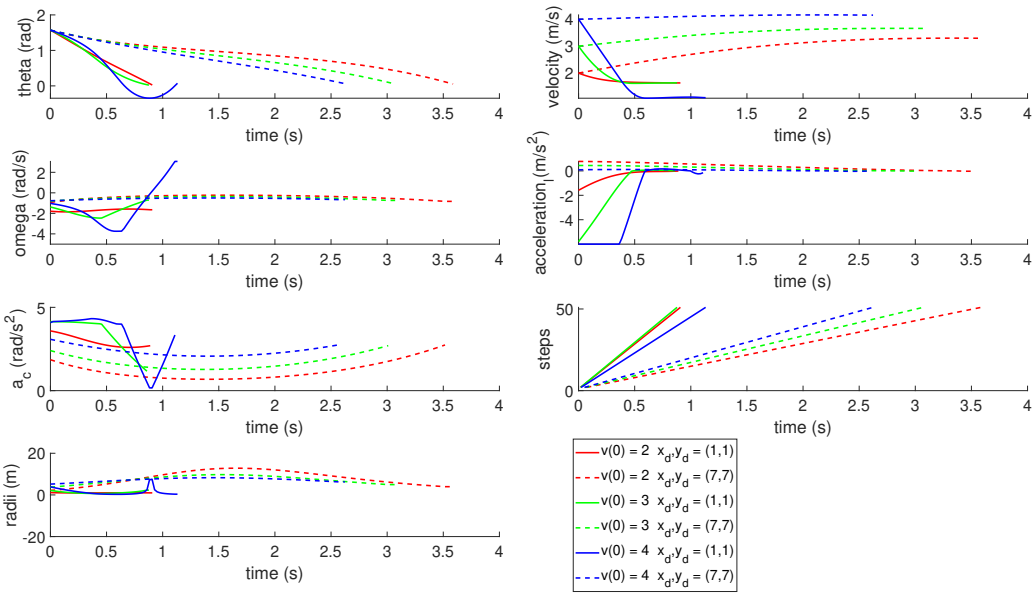

Figure 8: State variables result for turning scenario with different initial speeds and radii

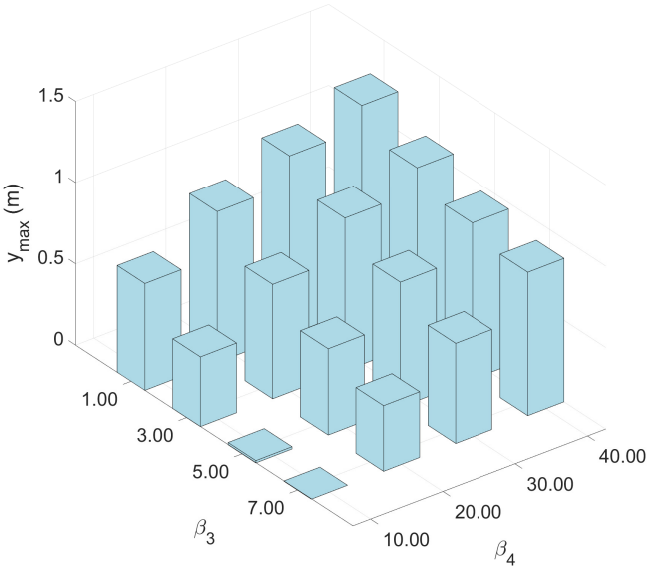

Figure 9: Deviation from the centerline with different β_4 and β_3

stretch or in space, e.g. when turning or approaching a red light. The costs considered by cyclists reflect multicriteria of travel efficiency, traffic rules, safety and physical efforts.

In the lane-keeping scenario, variations in β_5, which represents the weight of the cost associated with deviations from the center line, significantly influence the optimal trajectory. This parameter reflects cyclists' preference for maintaining proximity to the center of the bike lane. In turning scenarios, when centripetal acceleration approaches its upper limit, a smaller turning radius necessitates a reduction in linear velocity as angular velocity increases, under circumstances that initial and desired terminal speeds remain constant. This relationship underscores the critical balance between speed and angular velocity that cyclists must maintain to ensure stability and safety in turning. In the stationary obstacle avoidance scenario, the safety factor and the combined effects of β_3, and β_4 on trajectory deviation and velocity changes were analyzed. Additionally, compliance with the lane boundary rules influences avoidance patterns in complex obstacle scenarios.

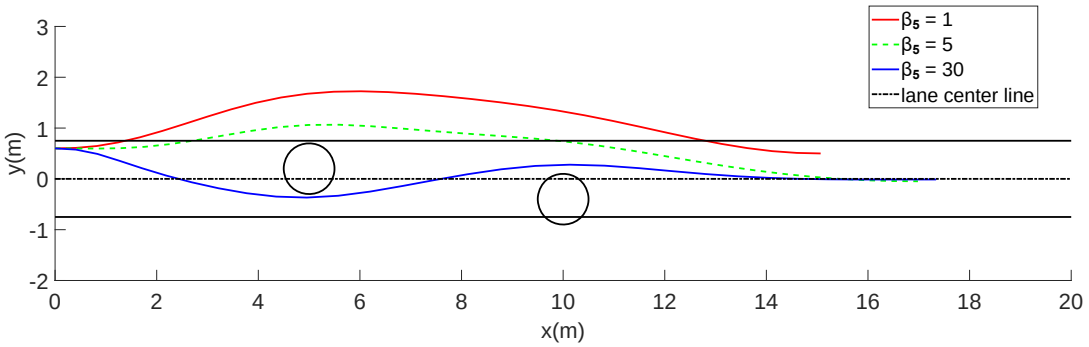

Figure 10: Optimal trajectory results for stationary obstacle avoidance scenario with different β_5

Future work will include calibration and validation of the model using real-world data. Additionally, uncertainty analyses of environmental observations and constraints will be conducted to further refine the model.

ACKNOWLEDGEMENTS

This work is funded by the Federal Ministry for Digital and Transport (BMDV) project PrioBike-HH (FKZ: I6DKVMOOIB).

References

Andersson, J. A. E., Gillis, J., Horn, G., Rawlings, J. B., & Diehl, M. (2019). CasADi – A software framework for nonlinear optimization and optimal control. *Mathematical Programming Computation*, *11*(1), 1–36. doi: 10.1007/s12532-018-0139-4

Helbing, D., & Molnar, P. (1995). Social force model for pedestrian dynamics. *Physical review E*, *51*(5), 4282.

Hoogendoorn, S., & Daamen, W. (2016). Bicycle headway modeling and its applications. *Transportation research record*, *2587*(1), 34–40.

Hoogendoorn, S., Gavriilidou, A., Daamen, W., & Duives, D. (2021). Game theoretical framework for bicycle operations: A multi-strategy framework. *Transportation Research Part C: Emerging Technologies*, *128*, 103175.

Mathew, T. V., Abdullah, O., Munigety, C. R., & Anirudha, S. (2012). *Strip-based simulation model for mixed traffic conditions* (Tech. Rep.).

Michon, J. A. (1985). A critical view of driver behavior models: what do we know, what should we do? In *Human behavior and traffic safety* (pp. 485–524). Springer.

Schmidt, C. M., Dabiri, A., Schulte, F., Happee, R., & Moore, J. K. (2023). Essential bicycle dynamics for microscopic traffic simulation: An example using the social force model. In *The evolving scholar-bmd 2023, 5th edition.*

Schönauer, R., Stubenschrott, M., Huang, W., Rudloff, C., & Fellendorf, M. (2012). Modeling concepts for mixed traffic: Steps toward a microscopic simulation tool for shared space zones. *Transportation research record*, *2316*(1), 114–121.

Twaddle, H., Schendzielorz, T., & Fakler, O. (2014). Bicycles in urban areas: Review of existing methods for modeling behavior. *Transportation research record*, *2434*(1), 140–146.

Wächter, A., & Biegler, L. T. (2006). On the implementation of an interior-point filter line-search algorithm for large-scale nonlinear programming. *Mathematical programming*, *106*, 25–57.

Yao, D., Zhang, Y., Li, L., Su, Y., Cheng, S., & Xu, W. (2009). Behavior modeling and simulation for conflicts in vehicles-bicycles mixed flow. *IEEE Intelligent Transportation Systems Magazine*, *1*(2), 25–30.